Ethanol Extract of *Maclura tricuspidata* Fruit Protects SH-SY5Y Neuroblastoma Cells against H₂O₂-Induced Oxidative Damage via Inhibiting MAPK and NF-κB Signaling

Weishun Tian [1], Suyoung Heo [1], Dae-Woon Kim [2], In-Shik Kim [1], Dongchoon Ahn [1], Hyun-Jin Tae [1], Myung-Kon Kim [2,*] and Byung-Yong Park [1,*]

[1] Bio-Safety Research Institute and College of Veterinary Medicine, Jeonbuk National University, Iksan 54596, Korea; tianws0502@126.com (W.T.); syheo@jbnu.ac.kr (S.H.); iskim@jbnu.ac.kr (I.-S.K.); ahndc@jbnu.ac.kr (D.A.); hjtae@jbnu.ac.kr (H.-J.T.)

[2] Department of Food Science and Technology, Jeonbuk National University, Jeonju 54896, Korea; eodns3344@gmail.com

* Correspondence: kmyuko@jbnu.ac.kr (M.-K.K.); parkb@jbnu.ac.kr (B.-Y.P.); Tel.: +82-63-270-4874 (B.-Y.P.)

Abstract: Free radical generation and oxidative stress push forward an immense influence on the pathogenesis of neurodegenerative diseases such as Alzheimer's disease and Parkinson's disease. *Maclura tricuspidata* fruit (MT) contains many biologically active substances, including compounds with antioxidant properties. The current study aimed to investigate the neuroprotective effects of MT fruit on hydrogen peroxide (H_2O_2)-induced neurotoxicity in SH-SY5Y cells. SH-SY5Y cells were pretreated with MT, and cell damage was induced by H_2O_2. First, the chemical composition and free radical scavenging properties of MT were analyzed. MT attenuated oxidative stress-induced damage in cells based on the assessment of cell viability. The H_2O_2-induced toxicity caused by ROS production and lactate dehydrogenase (LDH) release was ameliorated by MT pretreatment. MT also promoted an increase in the expression of genes encoding the antioxidant enzymes superoxide dismutase (SOD) and catalase (CAT). MT pretreatment was associated with an increase in the expression of neuronal genes downregulated by H_2O_2. Mechanistically, MT dramatically suppressed H_2O_2-induced Bcl-2 downregulation, Bax upregulation, apoptotic factor caspase-3 activation, Mitogen-activated protein kinase (MAPK) (JNK, ERK, and p38), and Nuclear factor-κB (NF-κB) activation, thereby preventing H_2O_2-induced neurotoxicity. These results indicate that MT has protective effects against H_2O_2-induced oxidative damage in SH-SY5Y cells and can be used to prevent and protect against neurodegeneration.

Keywords: *Maclura tricuspidata* (MT) fruit; neuroprotection; hydrogen peroxide; oxidative damage; MAPK; NF-κB

1. Introduction

Neurodegenerative diseases, including Parkinson's disease (PD) and Alzheimer's disease (AD), are caused mainly by neuronal damage, which is triggered by oxidative stress in many situations [1–4]. Endogenous ROS such as hydrogen peroxide (H_2O_2) has long been considered destructive molecules, which have been implicated in the pathogenesis of neurodegenerative diseases by causing oxidative stress and inducing apoptosis, and then promoting the pathological process of neurodegenerative diseases [5].

ROS can inactivate enzymes, oxidize proteins, damage DNA, cause lipid peroxidation, and denature proteins, disrupting cell function and integrity. They bring about neuronal injury, necrosis, and apoptosis, resulting in neurodegenerative diseases and loss of other functions [6,7]. ROS are mainly generated in mitochondria and accumulate during aging; therefore, limiting oxidative stress can be neuroprotective [8]. Activating the main antioxidant enzymes in the brain is an important method and mechanism to reduce neuronal

damage caused by oxidative stress [9]. Antioxidant enzymes such as superoxide dismutase (SOD), catalase (CAT), and peroxiredoxin family proteins scavenge superoxide and H_2O_2, thereby decreasing oxidative stress [5,10].

Regulatory proteins in the Bcl-2 family are important apoptosis-related factors and central moderators of cell death in H_2O_2-promoted oxidative stress [11]. Bcl-2 is an anti-apoptotic protein and forms a heterodimer with Bax, an apoptotic activator, thereby determining the fortune of cells [12]. Bax and Bcl-2 proteins are used commonly as indicators of cell survival and apoptosis, and their protein expression ratio (Bax/Bcl-2) can be used to assess cell status. Moreover, the cysteine protease caspase-3 is another vital protein involved in apoptosis that can be activated by H_2O_2 [13,14]. In summary, Bcl-2 upregulation, or cleaved-caspase-3 and Bax downregulation, can prevent neuronal apoptosis caused by oxidative stress.

Mitogen-activated protein kinase (MAPK) cascades are important signaling pathways that participate in various cellular processes including apoptosis, oxidative stress, proliferation, and stress responses. Previous studies have revealed that MAPK pathways are activated in neuroblastoma cells in response to H_2O_2 treatment [15,16]. In mammalian cells, there are three MAPK families: extracellular signal-regulated kinases (ERKs), C-Jun N-terminal kinases (JNKs), and p38 kinases. Abnormal levels of phosphorylated ERK, JNK, and p38 MAPKs have been found in the brains of Alzheimer's disease (AD) patients [17], suggesting that MAPKs participate in the pathogenesis of the neurodegenerative disease. Thus, understanding the biochemical processes surrounding H_2O_2-induced neuronal apoptosis can provide insight into the pathogenesis of neurodegenerative diseases and the effectiveness of treatments and explore alternative medicine for curing neurodegenerative disease.

Natural products contain a variety of active bioactive compounds that are good for health. The active ingredients in many herbal medicines have been verified to have neuroprotective effects by scavenging free radicals, thereby rejuvenating nerve cells from oxidative stress-induced damage [5,18,19]. MT is produced in high quantities in many Asia countries and is used as traditional medicine [20]. MT extracts and their active ingredients including vitamins, amino acids, and bioactive compounds such as rutin [21], anthocyanins [22], chlorogenic acid [23], and polysaccharides [24] have been verified to have antioxidant and neuroprotective effects. However, the underlying mechanism by which MT extracts exert their antioxidant effects is unknown. Our aim in this study was to explore the role of MT in H_2O_2-induced neurotoxicity and determine the underlying molecular mechanisms.

2. Results

2.1. HPLC Analysis of MT Extract

The chemical composition of MT fruit was evaluated using a Waters HPLC system. Peaks of polyphenolic compounds and parishin derivatives were observed (Figure 1B,D). The contents of polyphenolic compounds and parishin derivatives in the MT extract are shown in Table 1.
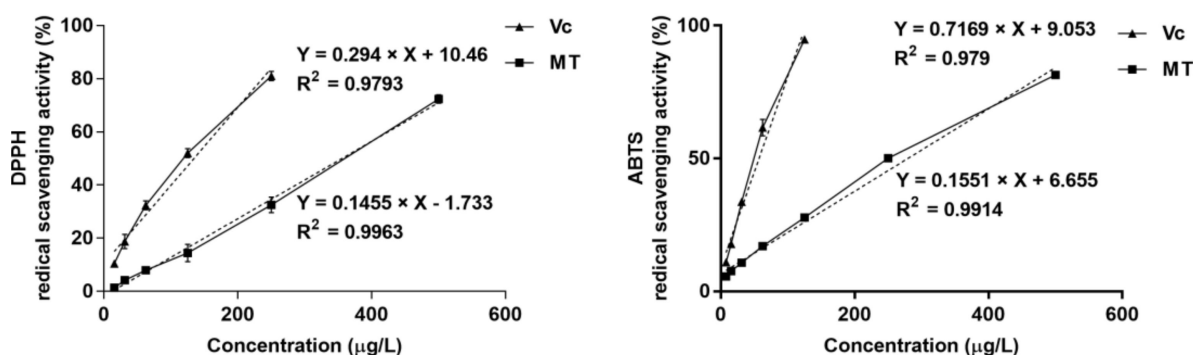
2.2. Radical Scavenging Activity of MT Extract

As shown in Figure 2 and Table 2, MT scavenged DPPH radicals in a concentration-dependent manner and was an active radical scavenger, with an IC_{50} value of 355.821 $\pm$ 8.343 µg/mL. MT also showed antioxidant activity in the ABTS assay, with an IC_{50} value of 278.741 $\pm$ 1.300 µg/mL.
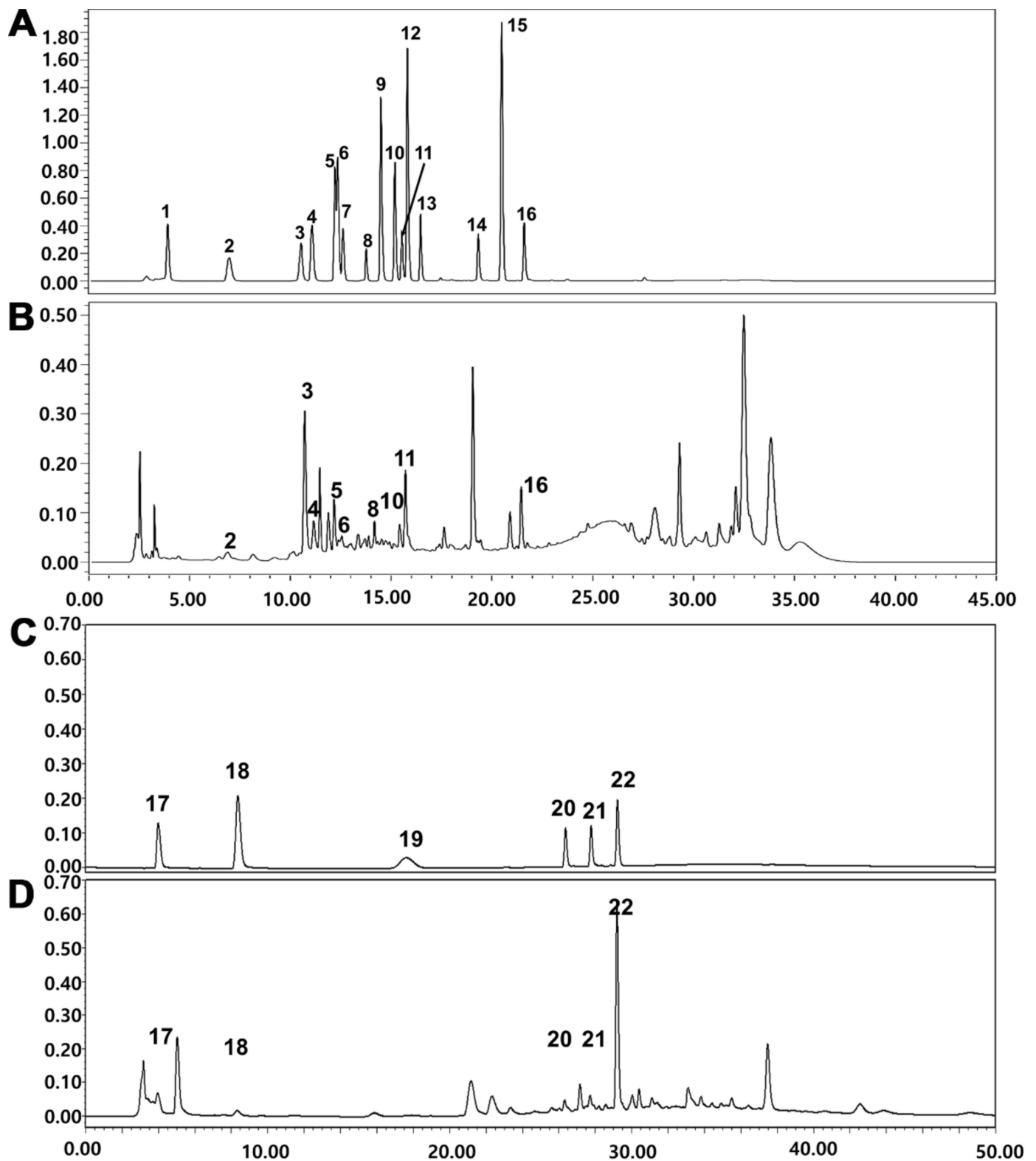
Figure 1. HPLC chromatograms of (**B**) polyphenolic compounds and (**D**) parishin derivatives of the 70% aqueous ethanol extract of MT. Mixtures of authentic standards for (**A**) polyphenolic compounds and (**C**) parishin derivatives: 1. gallic acid, 2. protocatechuic acid, 3. *p*-hydroxybenzoic acid, 4. chlorogenic acid, 5. caffeic acid, 6. syringic acid, 7. isovanillic acid, 8. rutin, 9. *p*-coumaric acid, 10. ferulic acid, 11. taxifolin, 12. trans-coumaric acid, 13. rosmarinic acid, 14. quercetin, 15. trans-cinnamic acid, 16. kaempferol, 17. gastrodin, 18. *p*-hydroxybenzyl alcohol, 19. parishin E, 20. parishin B, 21. parishin C, 22. parishin A.

Table 1. Polyphenolic compounds and parishin derivatives identified in a 70% aqueous ethanol extract of MT fruit.

Compounds	Concentration (g/g dw)
Protocatechuic acid	69.4 ± 1.3
p-Hydroxybenzoic acid	1066.8 ± 2.7
Chlorogenic acid	354.4 ± 0.9
Caffeic acid	57.4 ± 0.4
Syringic acid	84.5 ± 0.6
Isovanillic acid	128.9 ± 1.1
Rutin	223.0 ± 1.6
Taxifolin	87.7 ± 0.8
Quercetin	283.6 ± 1.3
Kaempferol	534.0 ± 0.3
Gastrodin	1296.5 ± 2.5
p-Hydroxybenzyl alcohol	215.8 ± 1.2
Parishin B	656.5 ± 2.1
Parishin C	1015.2 ± 1.5
Parishin A	7021.4 ± 3.5


Figure 2. DPPH and ABTS radical scavenging activity of MT extract. MT exhibited antioxidant activity with an IC_{50} of 355.821 ± 8.343 μg/mL for DPPH and 278.741 ± 1.300 μg/mL for ABTS. Data are expressed as mean ± SEM, *n* = 3.

Table 2. Effects of MT and ascorbic acid on DPPH and ABTS free radical scavenging assays.

Plant Extract/Standard	IC_{50} Value (μg/mL) of Radical Scavenging	
	DPPH Radical	**ABTS Radical**
MT extract	355.821 ± 8.343	278.741 ± 1.300
Ascorbic acid	134.501 ± 0.555	57.123 ± 0.873

Note: All data were expressed as the mean ± SEM, *n* = 3.

### 2.3. MT Improved H_2O_2-Induced Cell Damage in SH-SY5Y Cells

To investigate the protective effects of MT against H_2O_2-induced cytotoxicity in SH-SY5Y cells, cell viability was evaluated using MTT assays. First, the LC_{50} of H_2O_2 damage was determined to be 300 μM (Figure 3A). Cells were treated with MT (5–100 μg/mL) for 24 h to assess the cytotoxicity, and cell viability was significantly ($p < 0.001$) altered at the dose of 100 μg/mL (Figure 3B). The antioxidant effects of MT on H_2O_2-challenged cell damage were assessed. Cells were treated with non-toxic doses of MT for 2 h before exposure to 300 μM H_2O_2. H_2O_2 treatment alone significantly decreased cell viability, while pretreatment with MT at 5 to 50 μg/mL dramatically ($p < 0.05$, or $p < 0.001$) attenuated the H_2O_2-induced cytotoxicity, especially the dose of 50 μg/mL (Figure 3C). The protective effect of MT (20, 50 μg/mL) was supported by morphological observations. H_2O_2-challenged cells showed a shrunken appearance and a decrease in the number of neurites, and this was ameliorated by MT pretreatment (Figure 3D).
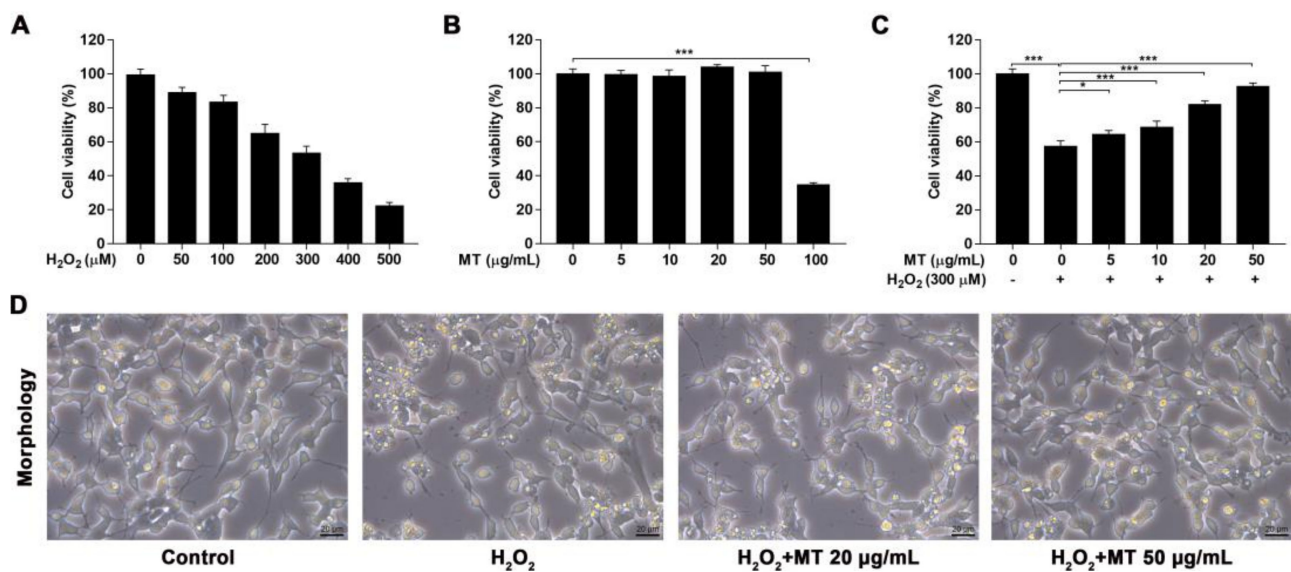
Figure 3. Protective effects of MT against H_2O_2-induced cell damage in SH-SY5Y cells. (**A**) SH-SY5Y cells were treated with various concentrations of H_2O_2 for 24 h, and LC_{50} (50% lethal concentration) was determined by MTT assay. (**B**) SH-SY5Y cells were treated with different concentrations of MT to assess cytotoxicity. (**C**) SH-SY5Y cells were pretreated with different concentrations of MT for 2 h before H_2O_2 treatment, and cell viability was measured. (**D**) Morphological changes (400×) were observed under an inverted microscope. Data are presented as mean ± SEM of three independent experiments. * $p < 0.05$, and *** $p < 0.001$.

### 2.4. MT Attenuated H_2O_2-Induced Nuclear Morphological Changes in SH-SY5Y Cells

To investigate nuclear morphological changes after pretreatment of SH-SY5Y cells with MT before exposure to H_2O_2, cells were stained with DAPI [25]. Control cells had regular oval-shaped nuclei, whereas H_2O_2-treated cells exhibited nuclear condensation (white arrow) and sporadic weaker staining (red arrow). Percentages of condensed nuclei and fragmented nuclei in the MT pretreatment groups were drastically ($p < 0.05$, or $p < 0.001$) decreased relative to that in the group not pretreated with MT, and there were fewer and less notable H_2O_2-induced nuclear morphological changes compared to those seen in cells exposed to H_2O_2 only (Figure 4).
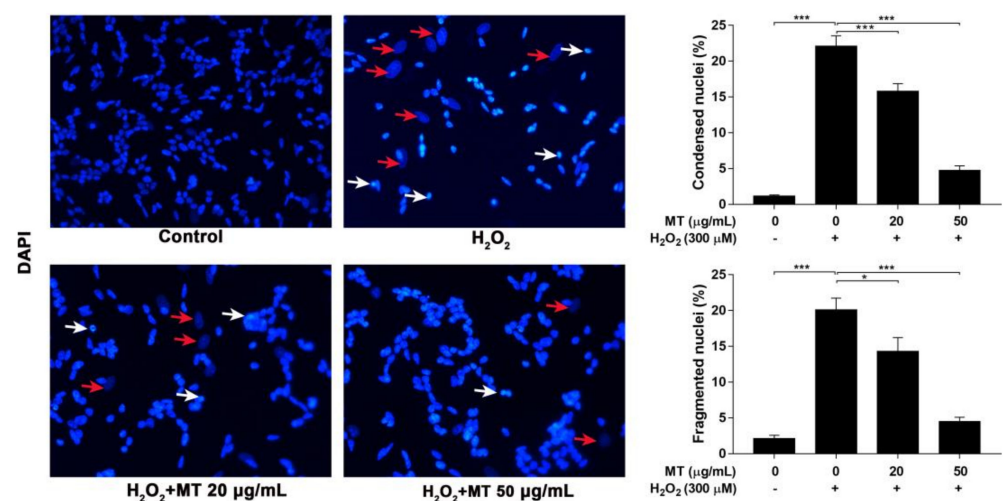
Figure 4. Effect of MT on H_2O_2-induced apoptosis in SH-SY5Y cells. Cells were pretreated with MT for 2 h following exposure to H_2O_2, percentages of condensed nuclei (white arrows) and fragmented nuclei (red arrows) were detected by DAPI staining (400×). Data are presented as mean ± SEM of three independent experiments. * $p < 0.05$, and *** $p < 0.001$.

2.5. MT Inhibited H$_2$O$_2$-Promoted ROS Production and LDH Leakage in SH-SY5Y Cells

ROS levels are indicators of oxidative stress, and excess ROS generation triggers cell apoptosis. LDH release level in media was measured as an index of cytotoxicity after exposure to H$_2$O$_2$. Compared with untreated control cells, cells challenged with H$_2$O$_2$ showed a markedly ($p < 0.001$) increased in ROS generation and LDH leakage, indicating that H$_2$O$_2$ treatment resulted in oxidative stress and cytotoxicity. However, pretreatment with MT significantly ($p < 0.05$, or $p < 0.001$) blocked the H$_2$O$_2$-challenged accumulation of ROS and release of LDH (Figure 5A,B). These results demonstrated that MT exerted protective effects on cells exposed to H$_2$O$_2$ by reducing oxidative stress and alleviating cytotoxicity.
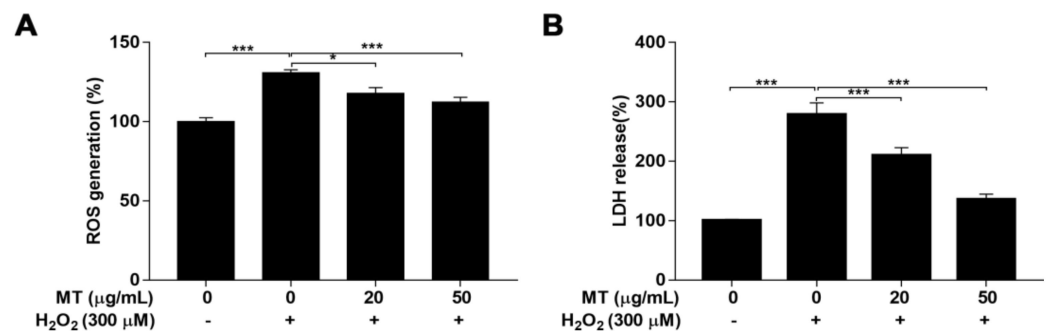
Figure 5. Effect of MT on H$_2$O$_2$-induced oxidative stress and cytotoxicity in SH-SY5Y cells. Cells were pretreated with MT for 2 h following exposure to H$_2$O$_2$. (**A**) ROS generation and (**B**) LDH release were assessed by ROS and LDH commercial kits according to the manufacturers' instructions. Data are presented as mean ± SEM of three independent experiments. * $p < 0.05$, and *** $p < 0.001$.

2.6. MT Increased the Expression of Antioxidant Enzymes in H$_2$O$_2$-Exposed SH-SY5Y Cells

Antioxidant enzymes, such as SOD and CAT, play important roles in maintaining an appropriate intracellular oxidation status. In this study, gene expression of SOD and CAT was examined, and treatment of cells with H$_2$O$_2$ resulted in a markedly ($p < 0.001$) decreased in gene expression of SOD and CAT. However, cells pretreated with MT followed by exposure to H$_2$O$_2$ demonstrated drastically ($p < 0.05$, or $p < 0.001$) higher gene expression of CAT and SOD than cells treated with H$_2$O$_2$ only (Figure 6A).
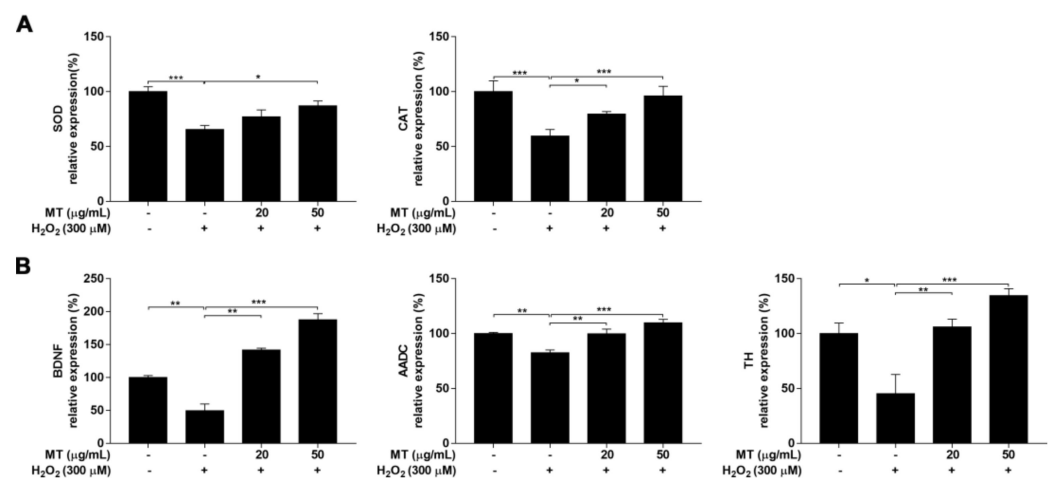
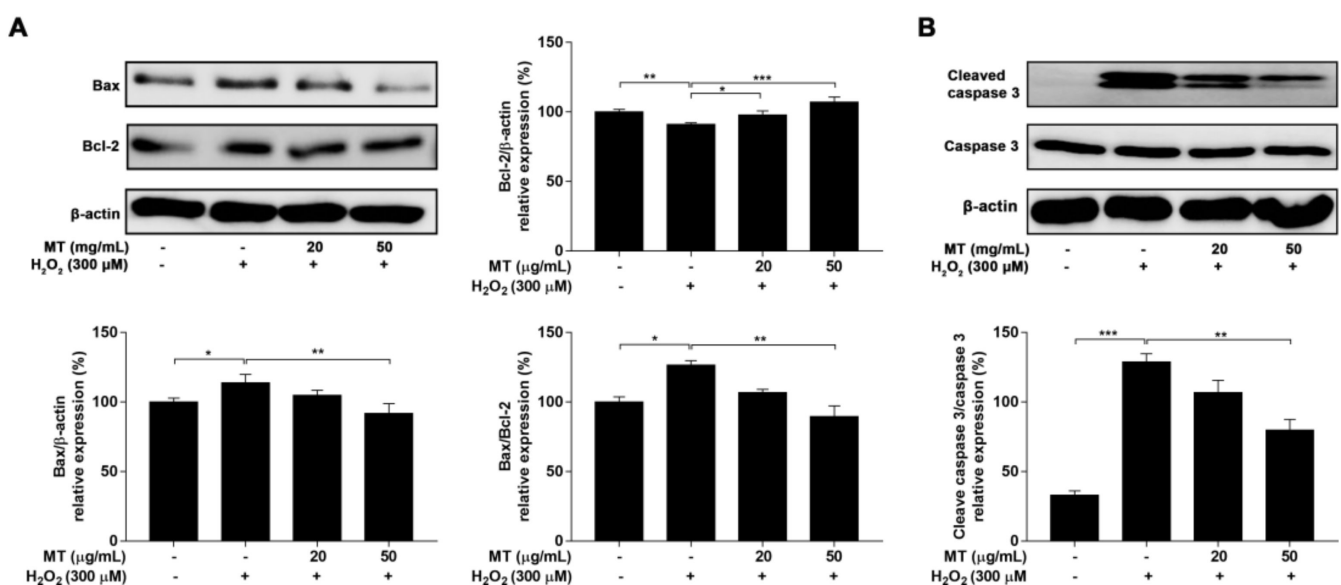**Figure 6.** Effects of MT on the expression of genes encoding antioxidant enzymes and neuronal markers in SH-SY5Y neuroblastoma cells. Expression of genes encoding the antioxidant enzymes (**A**) SOD and CAT and the neuronal markers (**B**) BDNF, AADC, and TH were evaluated by real-time PCR. Data are presented as mean ± SEM of three independent experiments. * $p < 0.05$, ** $p < 0.01$, and *** $p < 0.001$.

2.7. MT Elevated the Expression of Neuronal Biomarkers in Cells Exposed To H_2O_2

Gene expression of neuronal biomarkers including brain-derived neurotrophic factor (BDNF), aromatic L-amino acid decarboxylase (AADC), and tyrosine hydroxylase (TH) was assessed. Treatment of SH-SY5Y cells with H_2O_2 alone decreased the expression of the neuronal biomarkers BDNF, AADC, and TH ($p < 0.05$ or $p < 0.01$), but levels of these genes were similar ($p < 0.05$, $p < 0.01$, or $p < 0.001$) to those in control cells when SH-SY5Y cells were pre-treated with MT before exposure to H_2O_2 (Figure 6B).

2.8. MT Regulated H_2O_2-Induced Apoptosis-Related Proteins Expression

To further explore the mechanism of H_2O_2-challenged apoptosis, the expression of anti-apoptotic Bcl-2 and pro-apoptotic Bax was measured. Cells treated with H_2O_2 showed notable ($p < 0.05$, $p < 0.01$, or $p < 0.001$) upregulation of Bax expression and downregulation of Bcl-2 expression compared with the untreated group. Pretreatment with MT protected against the above effects of H_2O_2, as characterized by increased Bcl-2 expression and decreased Bax expression as well as a decreased Bax/Bcl-2 ratio (Figure 7A).


Figure 7. Effect of MT on the expression of apoptosis-related proteins in SH-SY5Y neuroblastoma cells. Expression levels of (**A**) Bcl-2, Bax, and (**B**) caspase-3 were analyzed by western blotting. Data are presented as mean ± SEM of three independent experiments. * $p < 0.05$, ** $p < 0.01$, and *** $p < 0.001$.

Caspase-3 plays a key role in neuronal apoptosis [26]. H_2O_2 induces the activation of caspase-3, which can enhance the process of apoptosis. As shown in Figure 7B, H_2O_2 treatment markedly elevated the expression of caspase-3, whereas pretreatment with MT significantly ($p < 0.05$, or $p < 0.001$) decreased the expression of caspase-3.

2.9. MT Attenuates Oxidative Stress via the MAPK and NF-κB Pathway

Previous studies have demonstrated that H_2O_2-challenged neurotoxicity can evoke cell death (apoptosis) via activation of MAPK family proteins [15,16]. Cells exposed to H_2O_2 alone showed increased ($p < 0.05$ or $p < 0.01$) expression of phosphorylated ERK, JNK, and p38 MAPK compared to control cells. Pretreatment with MT inhibited H_2O_2-induced activation of MAPK family proteins (Figure 8A–C). NF-κB p65 is a critical transcription factor that responds to H_2O_2-induced neuronal damage [27]. The level of phosphorylated NF-κB increased ($p < 0.001$) in H_2O_2-exposed cells. By contrast, MT pretreatment drastically ($p < 0.001$) protected against the H_2O_2-induced increase in phosphorylated NF-κB (Figure 8D). Taken together, these results indicate that MT is capable of protecting neuroblastoma cells from H_2O_2-induced damage by blocking MAPK and NF-κB signaling.
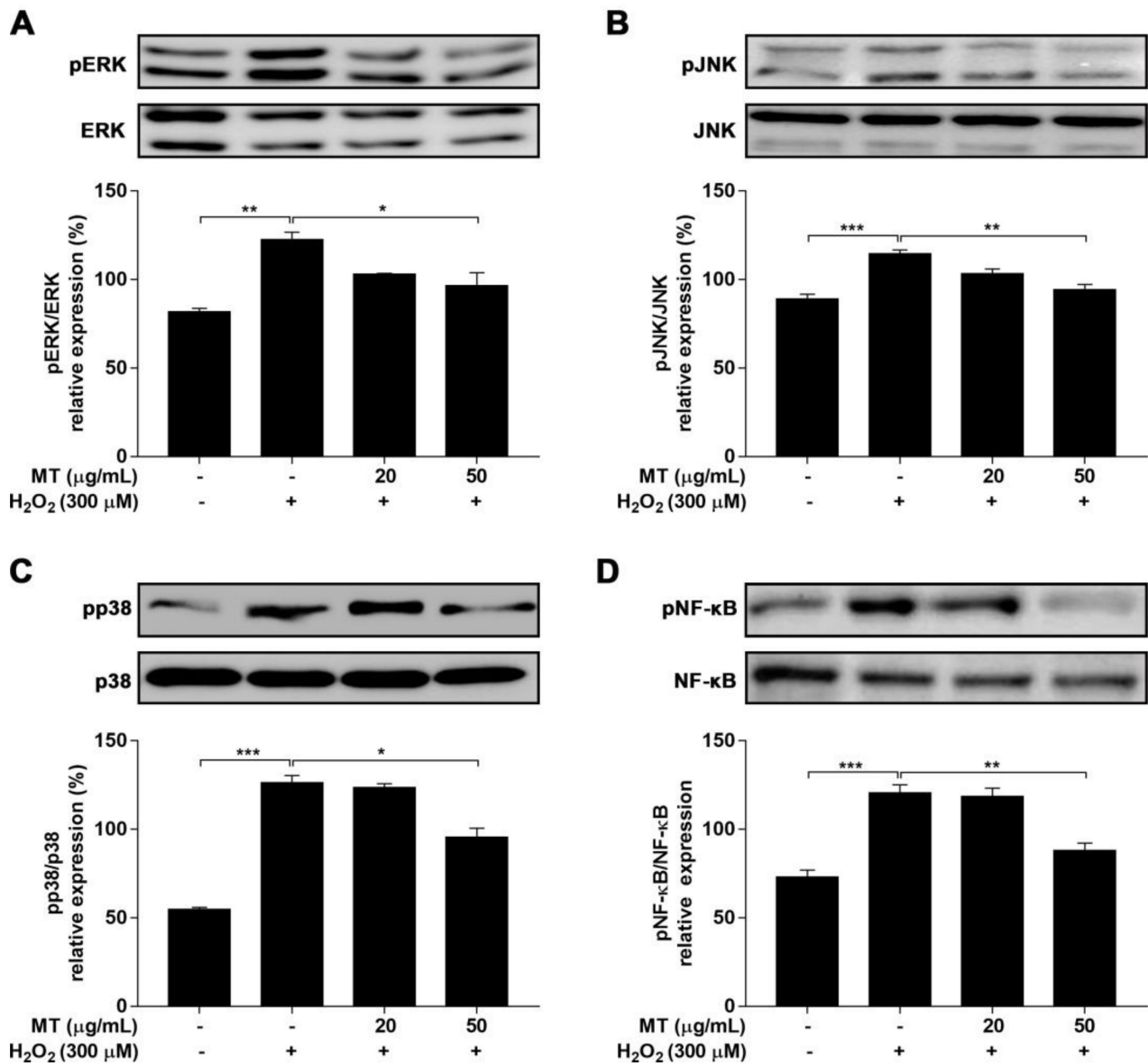
Figure 8. Effects of MT on MAPK (ERK, JNK, and p38) and NF-κB protein expression in SH-SY5Y neuroblastoma cells. Cells were pre-treated with MT for 2 h, followed by treatment with H_2O_2 for another 24 h. Expression levels of phosphorylated (**A–C**) MAPK family proteins and (**D**) NF-κB were evaluated by western blot analysis. Data are presented as mean ± SEM of three independent experiments. * $p < 0.05$ ** $p < 0.01$, and *** $p < 0.001$.

3. Discussion

Oxidative stress occurs as a result of an imbalance between production and accumulation of oxidants, including ROS, and is very toxic to cells and tissue [28,29]. Accumulation of ROS disturbs cellular homeostasis and activates a series of mechanisms that result in cell destruction. Oxidative stress has been implicated in neuronal cell death in several neurodegenerative diseases including Alzheimer's disease and Parkinson's disease. There is great interest in drugs that can reduce neurotoxicity induced by oxidative stress to help prevent and treat neurodegenerative disorders. Most natural medicines are rich in antioxidants and have limited side effects. In this case, looking for potential neuroprotective agents from natural products that can reduce neurotoxicity caused by oxidative stress may help prevent and treat neurodegenerative diseases [30]. Our purpose in this study was to explore the protective properties of MT on oxidative stress-induced neurotoxicity in SH-SY5Y cells and elucidate potential underlying mechanisms.

H_2O_2 is an oxidizing compound that functions as an oxidative stress inducer by increasing the production of ROS. H_2O_2-induced cytotoxicity is a common method used to investigate potential neuroprotective antioxidant effects of natural products [18,27]. Neural cells that are treated to H_2O_2 may suffer an apoptotic-like delayed death and necrosis. Exogenous H_2O_2 can pass through the cell membrane, thereby directly changing the intracellular homeostasis, which disturbs signal transduction and then causes DNA damage and cell apoptosis [31,32].

Apoptotic cell death is a programmed physiological process that is accompanied by morphological and biochemical alterations, including cell shrinkage, apoptotic body formation, nuclear condensation, activation of caspases, and chromosomal DNA fragmentation [33–35]. In the current study, morphology and DAPI staining showed that the morphology of cells and nuclei have changed after the cell was treated by H_2O_2 alone, and MT pretreatment alleviated the cytotoxicity induced by H_2O_2, which was further confirmed by MTT assay. Moreover, Intracellular ROS generation and LDH release are related to neuronal apoptosis and necrosis [5,36,37]. Overproduction of intracellular ROS can provoke mitochondrial dysfunction and neurodegeneration [38,39]. Fortunately, HPLC analysis revealed that MT contains many polyphenolic compounds and parishin derivatives, including rutin, caffeic acid, quercetin, and gastrodin (Table 1), all of which have strong antioxidant properties [40–42]. A previous study also showed that MT exists antioxidant activity [43]. Moreover, DPPH and ABTS assays revealed that MT has the antioxidant capacity and can scavenge free radicals to decrease oxidative stress, which in turn reduces H_2O_2-induced oxidative stress [44,45].

Accumulation of intracellular ROS or the destruction of antioxidant defense mechanism triggers physiological disorder and cell damage. Antioxidant enzymes such as SOD, CAT, and glutathione peroxidase (GPx) are active scavengers of superoxide and hydrogen peroxide. Previous studies have shown that the neuroprotective effects of some phytomedicines, such as MT extract, exist radical scavenging activity, enhance antioxidant enzyme activity, and increase the expression of the antioxidant enzymes CAT and SOD [43,46]. Furthermore, the bioactive compounds, such as protocatechuic acid, caffeic acid, rutin, and so on, can elevate the levels of the antioxidant enzyme [47–49]. MT can elevate the decrease in the gene expression of antioxidant enzymes induced by H_2O_2. Moreover, BDNF, TH, and AADC play critical roles in the neuronal survival, growth, and differentiation of dopaminergic (DArgic) neurons. Degeneration of these neurons in Parkinson's disease leads to catecholamine depletion and ultimately reduces dopamine levels in the substantia nigra [50]. MT attenuated H_2O_2-induced reduction in expression of BDNF, TH, and AADC. Hence, MT can protect human dopaminergic cells against oxidative stress through a variety of mechanisms to defense against the neurodegenerative disorders caused by oxidative stress. In summary, MT existed the ability to protect the SH-SY5Y cell from H_2O_2-induced neurotoxicity by enhancing the expression of antioxidant enzymes and neuronal biomarkers.

H_2O_2-induced apoptotic cell death in SH-SY5Y neuroblastoma cells is mediated by the intrinsic pathway of mitochondria through the activation of caspase [51]. The anti-apoptotic protein, Bcl-2, and pro-apoptotic, Bax, play important roles in the mitochondrial-related apoptosis pathway [25]. Bcl-2 family proteins govern apoptosis by regulating the permeability of the mitochondrial outer membrane [52]. Moreover, The Bcl-2 family protein mediates the apoptotic process through balancing pro-apoptotic (Bax) and anti-apoptotic (Bcl-2) expression, and their ratio (Bax/Bcl-2) is a functional indicator in regulating the apoptotic cell death [12]. In this study, H_2O_2-induced neurotoxicity slightly increased Bax and decreased Bcl-2 protein expression, all of which was reversed by MT pretreatment. Caspase-3, which is activated by H_2O_2, and is an apoptotic executor by triggering DNA fragments [18]. MT attenuated the activation of caspase 3 protein expression. In summary, MT can balance Bax and Bcl-2 protein expression and inhibit caspase-3 activation to protect against H_2O_2-induced neuronal damage.

MAPK cascades occupy an important role in transduction extracellular signals to cellular responses and modulate vital cellular processes such as proliferation, metabolism, stress responses, programmed death (apoptosis), and immune defense [53,54]. Oxidative stress triggered by ROS production can activate MAPK pathways, which can be monitored by assessing levels of phosphorylated ERK, JNK, and p38 MAPKs [18]. JNK1/2 and p38 MAPK pathways are usually activated by inflammatory cytokines and extracellular stressors such as UV light, heat, and ROS. Levels of phosphorylated JNK, p38, and ERK 1/2 MAPKs are increased in the postmortem brains of AD patients and inhibit their phosphorylation supply the methods to the treatment of AD [55,56]. Previous studies reported that many bioactive compounds isolated from MT could inhibit MAPK phosphorylation and exist neuroprotective effects [57,58]. Similarly, the current study revealed MT pretreatment notably prevented the H_2O_2-induced increases in levels of phosphorylated ERK, JNK, and p38 MAPKs. NF-κB is a protein complex that controls transcription of DNA, cytokine production, and cell survival and plays an important role in neurodegenerative diseases [59]. The activation of NF-κB is considered to be part of the stress response, and it can be activated by a variety of stimuli including oxidative stress. H_2O_2 can rapidly activate NF-κB, which participates in ROS-induced cell death [60]. MT effectively inhibited H_2O_2-induced phosphorylation of NF-κB. Thus, MT protected SH-SY5Y neuroblastoma cells from H_2O_2-evoked apoptosis by inhibiting MAPK and NF-κB signaling.

4. Materials and Methods

4.1. Chemicals

Polyphenolic compounds, 3-(4,5-dimethylthiazol-2-yl) -2,5-diphenyltetrazolium bromide (MTT), 2, 2′-azino-bis (3-ethylbenzthiazoline-6-sulfonic acid) disodium salt (ABTS), fluorometric intracellular ROS kit, penicillin/streptomycin, and 2-(4-amidinophenyl)-6-indolecarbami dine dihydrochloride (DAPI) were purchased from Sigma-Aldrich (St. Louis, MO, USA). Parishin derivatives were bought from Chengdu Biopurify Phytochemicals Ltd. (Chengdu, Sichuan, China). Fetal bovine serum (FBS) was obtained from Young in Frontier Company (Seoul, Korea). 2,2-Diphenyl-1-picrylhydrazyl (DPPH) was bought from MedChemExpress (Princeton, NJ, USA). Ham's F-12 Nutrient Mix medium, BCA protein assay kit, and cDNA synthesis kit (ReverTra Ace qPCR RT Kit) were purchased from Thermo Fisher Scientific (Waltham, MA, USA). Eagle's Minimum Essential Medium (EMEM) was obtained from ATCC (Manassas, VA, USA). H_2O_2 was purchased from Fujifilm Wako Pure Chemical (Osaka, Japan). The SYBR green qPCR Kit was supplied by TOYOBO (Osaka, Japan). Lactate dehydrogenase (LDH) cytotoxicity assay kit was bought from TAKARA (Shiga Prefecture, Japan). Clarity western chemiluminescent (ECL) substrate kit was supplied by Bio-Rad Laboratories (Hercules, CA, USA).

4.2. MT Fruit Collection and Extract Preparation

Fully ripe MT was purchased in early November 2019, from a farm located in Sunchang district (Jeonbuk, Korea). An MT specimen was stored at the Herbarium of the Department of Food Science and Technology, College of Agricultural Life Science, Jeonbuk National University, Korea.

Powdered MT fruit (100 g) was extracted in 70% aqueous ethanol mixture (500 mL) at room temperature for 20 min using a sonicator (Hwa Shin Instrument Co., Seoul, Korea) and centrifuged ($4500\times g$, 10 min). The medicinal residue was re-extracted twice as described above. Supernatants from the three extractions were combined and vacuum evaporated to remove ethanol at 40 °C. The obtained MT extract was freeze-dried.

4.3. High-Performance Liquid Chromatography (HPLC) Analysis

HPLC analysis of polyphenolic compounds was performed using a Waters HPLC system (Milford, MA, USA) consisting of a 2690 separation module and 996 photodiode array detector (PDA) with a ZORBAX Eclipse XDB-C18 column (250 mm × 4.6 mm, 5 μm; Agilent Technologies, Inc., Santa Clara, CA, USA). The mobile phase consisted of solvent A

(0.1% formic acid and 10% acetonitrile in deionized water) and solvent B (0.1% formic acid and 10% deionized water in acetonitrile). The ratio of the mobile phase was maintained at A:B = 100:0 (0–5 min), 83:17 (5–10 min), 80:20 (10–30 min), and 100:0 (30–35 min) at a flow rate of 1.0 mL/min. UV–VIS absorption spectra were recorded at 200–400 nm during HPLC analysis, and polyphenolic compounds were measured at 280 nm. To analyze parishin derivatives, the mobile phase consisted of 0.1% phosphoric acid in deionized water (solvent A) and 0.1% phosphoric acid in methanol (solvent B). The mobile phase was used at A:B = 85:15 (0–5 min), 45:55 (5–20 min), and 85:15 (20–35 min) at a flow rate of 0.8 mL/min. UV–VIS absorption spectra were recorded from 200–400 nm during HPLC analysis, and parishin derivatives were detected at 220 nm. Identification of compounds was based on comparisons of HPLC retention time and UV profiles with those of authentic standards. Quantification of individual compounds was based on calibration curves prepared from serial dilutions of stock solution (1000 µg/mL).

4.4. Radical Scavenging Properties of MT Extract

DPPH and ABTS assays are convenient and popular to apply the radical scavenging properties of compounds. The radical scavenging properties of MT fruit extract were evaluated as described previously [61].

DPPH and ABTS radical scavenging levels (%) were acquired using the following Formula (1):

$$\text{Radical scavenging level } (\%) = \frac{A \text{ control} - A \text{ sample}}{A \text{ control}} \times 100 \tag{1}$$

Radical scavenging properties of MT are presented as half-maximal inhibitory concentration (IC_{50}) (µg/mL).

4.5. Cell Culture

Human dopaminergic neuroblastoma SH-SY5Y cells were obtained from Korean Cell Line Bank (KCLB), and cultured in EMEM/F12 (1:1) mixture supplemented with 10% FBS and antibiotics in a 5% CO_2 humidified incubator at 37 °C. SH-SY5Y cells were sub-cultured or seeded into plates until approximately 90% confluence.

4.6. Cell Cytotoxicity Assay and Morphological Observations

SH-SY5Y neuroblastoma cells were seeded into 96-well plates at a density of 1×10^4 cells/well. To evaluate the cytotoxicity of MT extract and 50% lethal concentration (LC_{50}) of H_2O_2, MT (5–100 µg/mL) or H_2O_2 (50–500 µM) was treated with cells for 24 h. To induce oxidative stress, cells were pretreated with different concentrations of MT for 2 h and then co-cultured with freshly prepared H_2O_2 (LC_{50}) for 24 h. Cell viability was assayed with the MTT method. In addition, images of cells were captured under an inverted microscope (400×) equipped with a camera (CKX41, Olympus Corporation, Shinjuku City, Japan) for morphological analysis.

4.7. DAPI Staining

Changes in the morphology of the nucleus of cells after H_2O_2 treatment were evaluated by 4, 6-diamidino 2-phenylindole dihydrochloride (DAPI) staining. SH-SY5Y cells were placed in a 24-well plate containing gelatin-coated coverslips. Cells from different treatment groups were processed and fixed with 4% paraformaldehyde (PFA) for 20 min at room temperature. Fixed cells were washed twice and permeabilized with 0.25% Triton X-100 in PBS for 10 min. Cells were incubated with fresh diluted DAPI (300 µM) solution for 5 min at room temperature.

Samples were rinsed with PBS and then water. Coverslips were removed from the wells carefully and mounted using mounting medium onto microscope slides. Stained cells were examined under a Leica DM2500 fluorescence microscope (Leica Microsys-

tems, Wetzlar, Germany) at $400\times$ magnification, and percentages of condensed nuclei and fragmented nuclei were calculated.

4.8. Intracellular ROS Production and Lactate Dehydrogenase (LDH) Release Assay

Intracellular ROS generation was detected using a fluorometric intracellular ROS Kit according to the manufacturer's instructions. Briefly, SH-SY5Y cells were plated at a density of 1.0×10^4 cells/well in 96-well plates overnight, pretreated with MT (5, 10, 20, and 50 mg/mL) for 2 h, and then co-treated with H_2O_2 for 3 h. Cells washed by Hanks' Balanced Salt Solution (HBSS). The master reaction mix (100 µL) was added and then cells were incubated for 30 min in an incubator (5% CO_2, 37 °C). The fluorescence intensity was measured at an excitation of 640 nm and an emission of 675 nm.

The release of LDH from cells was measured using an LDH cytotoxicity detection assay kit according to the manufacturer's instructions. SH-SY5Y cells were plated at a density of 1.0×10^4 cells/well in 96-well plates overnight, pretreated with MT (5, 10, 20, and 50 mg/mL) for 2 h, and then co-treated with H_2O_2 for 24 h. The supernatant was collected after 24 h, and LDH relative levels were detected by determining the absorbance at 490 nm with an automated microplate reader.

4.9. RNA Extraction and Quantitative Real-Time PCR (qPCR) Analysis

Total cellular RNA was isolated from cells with a commercial total RNA extraction kit (GeneAll, Seoul, Korea) according to the manufacturer's instructions. cDNA was reverse-transcribed from 3 µg total RNA using the RevertAid First Strand cDNA Synthesis Kit according to the manufacturer's instructions. Quantitative real-time PCR (qPCR) was performed on a CFX96 Real-Time PCR Detection System (Bio-Rad Laboratories, Hercules, CA, USA) with SYBR Green I as double-stranded DNA-specific binding dye. Specificity was verified by melting curve analysis. Quantification was performed by normalizing the *Ct* values of each sample to that of glyceraldehyde-3-phosphate dehydrogenase (GAPDH) as an internal control. All PCR primers were obtained from Bioneer (Daejeon, Korea) (Table 3).

Table 3. Sequences of primers using in this study.

Gene Target	Primer Name	Primer Sequence (5′-3′)
SOD	SOD F	AGGCCGTGTGCGTGCTGAAG
	SOD R	CACCTTTGCCCAAGTCATCTGC
CAT	CAT F	CCTTTCTGTTGAAGATGCGGCG
	CAT R	GGCGGTGAGTGTCAGGATAG
TH	TH F	GAGGAGAAGGAGGGGAAG
	TH R	ACTCAAACACCTTCACAGCT
AADC	AAD F	AACAAAGTGAATGAAGCTCTTC
	AAD R	GCTCTTTGATGTGTTCCCAG
BDNF	BDNF F	ATGACCATCCTTTTCCTTACT
	BDNF R	GCCACCTTGTCCTCGGAT
GAPDH	GAPDH F	TTCACCACCATGGAGAAGGC
	GAPDH R	GGCATGGACTGTGGTCATGA

Note: SOD, Superoxide dismutase; CAT, Catalase; TH, Tyrosine hydroxylase; AADC, Amino acid decarboxylase; BDNF, Brain-derived neurotrophic factor; GAPDH, Glyceraldehyde 3-phosphate dehydrogenase.

4.10. Western Blot Analysis

SH-SY5Y cells were pretreated with MT (20 and 50 µg/mL) for 2 h and then co-incubated with H_2O_2 for 24 h. Cells were lysed with radioimmunoprecipitation assay (RIPA) buffer. The supernatant was collected after centrifugation at $13,000\times g$ for 15 min at 4 °C. Equal amounts of proteins were loaded on 10–12% sodium dodecyl sulfate-polyacrylamide gels for electrophoresis (SDS-PAGE) and then transferred onto nitrocellulose membranes. Membranes were incubated in 5% non-fat dry milk in Tris-buffered saline with Tween-20 (TBST) at room temperature for 2 h. Primary antibodies were added, and membranes were incubated at 4 °C overnight after three washes. The primary antibodies

listed in Table 4 were used according to the manufacturers' specifications. Membranes were washed three times with TBST and then incubated with secondary antibodies (goat anti-rabbit IgG-HRP) for 2 h. Bands were visualized using a Clarity Western Chemiluminescent (ECL) substrate kit, and band images were obtained using the LAS 500 imaging system (GE Healthcare, Chicago, IL, USA). Bands were quantified using Quantity One software (Bio-Rad Laboratories, Hercules, CA, USA).

Table 4. Primary antibodies were used in this study.

Antibody	Host	Manufacturer	Cat. No.	Dilution
Bcl-2	Rabbit	Cell Signaling Technology, Danvers, MA, USA	3498	1:1000
Bax	Rabbit	Santa Cruz Biotechnology, Dallas, TX, USA	sc-493	1:500
Cleave caspase 3	Rabbit	Cell Signaling Technology, Danvers, MA, USA	9661	1:1000
Caspase 3	Rabbit	Cell Signaling Technology, Danvers, MA, USA	9665	1:1000
p-JNK	Rabbit	Cell Signaling Technology, Danvers, MA, USA	9251	1:1000
JNK	Rabbit	Cell Signaling Technology, Danvers, MA, USA	9252	1:1000
p-ERK	Rabbit	Cell Signaling Technology, Danvers, MA, USA	9101	1:1000
ERK	Rabbit	Cell Signaling Technology, Danvers, MA, USA	9102	1:1000
p-p38	Rabbit	Cell Signaling Technology, Danvers, MA, USA	9211	1:1000
p38	Rabbit	Cell Signaling Technology, Danvers, MA, USA	9212	1:1000
p-NF-κB	Rabbit	Cell Signaling Technology, Danvers, MA, USA	3033	1:1000
NF-κB	Rabbit	Cell Signaling Technology, Danvers, MA, USA	8242	1:1000
β-actin	Rabbit	Cell Signaling Technology, Danvers, MA, USA	4970	1:1000

4.11. Statistical Analysis

All data are expressed as mean $\pm$ standard error of the mean (SEM). Group comparisons were performed using one-way analysis of variance (ANOVA) in Prism 7.0 (GraphPad Software Inc., San Diego, CA, USA). A value of $p < 0.05$ was considered statistically significant.

5. Conclusions

Taken together, our results demonstrate that MT can attenuate H_2O_2-induced neurotoxicity in SH-SY5Y cells. MT suppressed intracellular ROS generation and LDH leakage and increased the expression of genes encoding antioxidant enzymes as well as proteins involved in brain function and neurotransmitter synthesis. Furthermore, MT regulated the expression of apoptosis-related proteins (Bcl-2, Bax, and caspase 3), while pretreatment of cells with MT blocked the H_2O_2-induced phosphorylation of MAPK/NF-κB signaling pathway proteins. MT is a promising therapeutic agent for the treatment of neurodegenerative diseases.

Author Contributions: W.T. and S.H. contributed equally to this work. Conceptualization, W.T., S.H., M.-K.K. and B.-Y.P.; methodology, W.T., S.H., M.-K.K. and B.-Y.P.; software, W.T. and S.H.; writing—original draft preparation, W.T. and S.H.; writing—review and editing, D.-W.K., I.-S.K., D.A., H.-J.T., M.-K.K. and B.-Y.P.; supervision, M.-K.K. and B.-Y.P. All authors have read and agreed to the published version of the manuscript.

Institutional Review Board Statement: Not applicable.

Informed Consent Statement: Not applicable.

Data Availability Statement: Not applicable.

Conflicts of Interest: The authors declare no conflict of interest.

References

1. Choi, J.; Sullards, M.C.; Olzmann, J.A.; Rees, H.D.; Weintraub, S.T.; Bostwick, D.E.; Gearing, M.; Levey, A.I.; Chin, L.S.; Li, L. Oxidative damage of DJ-1 is linked to sporadic Parkinson and Alzheimer diseases. *J. Biol. Chem.* **2006**, *281*, 10816–10824. [CrossRef]
2. Caviness, J.N.; Lue, L.; Adler, C.H.; Walker, D.G. Parkinson's disease dementia and potential therapeutic strategies. *CNS Neurosci. Ther.* **2011**, *17*, 32–44. [CrossRef]
3. Stoy, N.; Mackay, G.M.; Forrest, C.M.; Christofides, J.; Egerton, M.; Stone, T.W.; Darlington, L.G. Tryptophan metabolism and oxidative stress in patients with Huntington's disease. *J. Neurochem.* **2005**, *93*, 611–623. [CrossRef]
4. Kim, G.H.; Kim, J.E.; Rhie, S.J.; Yoon, S. The Role of Oxidative Stress in Neurodegenerative Diseases. *Exp. Neurobiol.* **2015**, *24*, 325–340. [CrossRef]
5. Nirmaladevi, D.; Venkataramana, M.; Chandranayaka, S.; Ramesha, A.; Jameel, N.M.; Srinivas, C. Neuroprotective effects of bikaverin on H2O2-induced oxidative stress mediated neuronal damage in SH-SY5Y cell line. *Cell. Mol. Neurobiol.* **2014**, *34*, 973–985. [CrossRef] [PubMed]
6. Nita, M.; Grzybowski, A. The Role of the Reactive Oxygen Species and Oxidative Stress in the Pathomechanism of the Age-Related Ocular Diseases and Other Pathologies of the Anterior and Posterior Eye Segments in Adults. *Oxid. Med. Cell. Longev.* **2016**, *2016*, 3164734. [CrossRef]
7. Valko, M.; Leibfritz, D.; Moncol, J.; Cronin, M.T.; Mazur, M.; Telser, J. Free radicals and antioxidants in normal physiological functions and human disease. *Int. J. Biochem. Cell Biol.* **2007**, *39*, 44–84. [CrossRef] [PubMed]
8. Zadori, D.; Klivenyi, P.; Szalardy, L.; Fulop, F.; Toldi, J.; Vecsei, L. Mitochondrial disturbances, excitotoxicity, neuroinflammation and kynurenines: Novel therapeutic strategies for neurodegenerative disorders. *J. Neurol. Sci.* **2012**, *322*, 187–191. [CrossRef]
9. Lau, F.C.; Shukitt-Hale, B.; Joseph, J.A. The beneficial effects of fruit polyphenols on brain aging. *Neurobiol. Aging* **2005**, *26* (Suppl. 1), 128–132. [CrossRef] [PubMed]
10. Kim, Y.; Jang, H.H. Role of Cytosolic 2-Cys Prx1 and Prx2 in Redox Signaling. *Antioxidants* **2019**, *8*, 169. [CrossRef]
11. Ku, B.; Liang, C.; Jung, J.U.; Oh, B.H. Evidence that inhibition of BAX activation by BCL-2 involves its tight and preferential interaction with the BH3 domain of BAX. *Cell Res.* **2011**, *21*, 627–641. [CrossRef]
12. Youle, R.J.; Strasser, A. The BCL-2 protein family: Opposing activities that mediate cell death. *Nat. Rev. Mol. Cell Biol.* **2008**, *9*, 47–59. [CrossRef] [PubMed]
13. Martin, D.; Salinas, M.; Fujita, N.; Tsuruo, T.; Cuadrado, A. Ceramide and reactive oxygen species generated by H2O2 induce caspase-3-independent degradation of Akt/protein kinase B. *J. Biol. Chem.* **2002**, *277*, 42943–42952. [CrossRef]
14. Zhao, X.; Fang, J.; Li, S.; Gaur, U.; Xing, X.; Wang, H.; Zheng, W. Artemisinin Attenuated Hydrogen Peroxide (H2O2)-Induced Oxidative Injury in SH-SY5Y and Hippocampal Neurons via the Activation of AMPK Pathway. *Int. J. Mol. Sci.* **2019**, *20*, 2680. [CrossRef] [PubMed]
15. Kwon, S.H.; Kim, J.A.; Hong, S.I.; Jung, Y.H.; Kim, H.C.; Lee, S.Y.; Jang, C.G. Loganin protects against hydrogen peroxide-induced apoptosis by inhibiting phosphorylation of JNK, p38, and ERK 1/2 MAPKs in SH-SY5Y cells. *Neurochem. Int.* **2011**, *58*, 533–541. [CrossRef] [PubMed]
16. Fan, Z.; Wang, X.; Zhang, M.; Zhao, C.; Mei, C.; Li, P. MAPK Pathway Inhibitors Attenuated Hydrogen Peroxide Induced Damage in Neural Cells. *Biomed. Res. Int.* **2019**, *2019*, 5962014. [CrossRef]
17. Zhu, X.; Lee, H.G.; Raina, A.K.; Perry, G.; Smith, M.A. The role of mitogen-activated protein kinase pathways in Alzheimer's disease. *Neurosignals* **2002**, *11*, 270–281. [CrossRef]
18. Lee, K.M.; Lee, A.S.; Choi, I. Melandrii Herba Extract Attenuates H2O2-Induced Neurotoxicity in Human Neuroblastoma SH-SY5Y Cells and Scopolamine-Induced Memory Impairment in Mice. *Molecules* **2017**, *22*, 1646. [CrossRef]
19. Lee, H.J.; Spandidos, D.A.; Tsatsakis, A.; Margina, D.; Izotov, B.N.; Yang, S.H. Neuroprotective effects of Scrophularia buergeriana extract against glutamate-induced toxicity in SH-SY5Y cells. *Int. J. Mol. Med.* **2019**, *43*, 2144–2152. [CrossRef]
20. Yuan, Q.; Zhao, L. The Mulberry (*Morus alba* L.) Fruit-A Review of Characteristic Components and Health Benefits. *J. Agric. Food Chem.* **2017**, *65*, 10383–10394. [CrossRef] [PubMed]
21. Park, S.E.; Sapkota, K.; Choi, J.H.; Kim, M.K.; Kim, Y.H.; Kim, K.M.; Kim, K.J.; Oh, H.N.; Kim, S.J.; Kim, S. Rutin from Dendropanax morbifera Leveille protects human dopaminergic cells against rotenone induced cell injury through inhibiting JNK and p38 MAPK signaling. *Neurochem. Res.* **2014**, *39*, 707–718. [CrossRef]
22. Kelsey, N.; Hulick, W.; Winter, A.; Ross, E.; Linseman, D. Neuroprotective effects of anthocyanins on apoptosis induced by mitochondrial oxidative stress. *Nutr. Neurosci.* **2011**, *14*, 249–259. [CrossRef] [PubMed]
23. Shan, S.; Tian, L.; Fang, R. Chlorogenic Acid Exerts Beneficial Effects in 6-Hydroxydopamine-Induced Neurotoxicity by Inhibition of Endoplasmic Reticulum Stress. *Med. Sci. Monit.* **2019**, *25*, 453–459. [CrossRef]
24. Yang, J.; Shao, X.; Wang, L.; Xu, H.; Sun, Y.; Jiang, J.; Sun, L. Angelica polysaccharide exhibits antitumor effect in neuroblastoma cell line SH-SY5Y by up-regulation of miR-205. *Biofactors* **2019**. [CrossRef] [PubMed]
25. Han, S.M.; Kim, J.M.; Park, K.K.; Chang, Y.C.; Pak, S.C. Neuroprotective effects of melittin on hydrogen peroxide-induced apoptotic cell death in neuroblastoma SH-SY5Y cells. *BMC Complement. Altern. Med.* **2014**, *14*, 286. [CrossRef]
26. Hartmann, A.; Hunot, S.; Michel, P.P.; Muriel, M.P.; Vyas, S.; Faucheux, B.A.; Mouatt-Prigent, A.; Turmel, H.; Srinivasan, A.; Ruberg, M.; et al. Caspase-3: A vulnerability factor and final effector in apoptotic death of dopaminergic neurons in Parkinson's disease. *Proc. Natl. Acad. Sci. USA* **2000**, *97*, 2875–2880. [CrossRef] [PubMed]

27. Chetsawang, B.; Putthaprasart, C.; Phansuwan-Pujito, P.; Govitrapong, P. Melatonin protects against hydrogen peroxide-induced cell death signaling in SH-SY5Y cultured cells: Involvement of nuclear factor kappa B, Bax and Bcl-2. *J. Pineal Res.* **2006**, *41*, 116–123. [CrossRef]

28. Sorg, O. Oxidative stress: A theoretical model or a biological reality? *Comptes R. Biol.* **2004**, *327*, 649–662. [CrossRef]

29. Gilgun-Sherki, Y.; Rosenbaum, Z.; Melamed, E.; Offen, D. Antioxidant therapy in acute central nervous system injury: Current state. *Pharmacol. Rev.* **2002**, *54*, 271–284. [CrossRef]

30. Pandareesh, M.D.; Mythri, R.B.; Srinivas Bharath, M.M. Bioavailability of dietary polyphenols: Factors contributing to their clinical application in CNS diseases. *Neurochem. Int.* **2015**, *89*, 198–208. [CrossRef]

31. Bienert, G.P.; Schjoerring, J.K.; Jahn, T.P. Membrane transport of hydrogen peroxide. *Biochim. Biophys. Acta* **2006**, *1758*, 994–1003. [CrossRef]

32. Giorgio, M.; Trinei, M.; Migliaccio, E.; Pelicci, P.G. Hydrogen peroxide: A metabolic by-product or a common mediator of ageing signals? *Nat. Rev. Mol. Cell Biol.* **2007**, *8*, 722–728. [CrossRef] [PubMed]

33. Fernandez-Segura, E.; Canizares, F.J.; Cubero, M.A.; Warley, A.; Campos, A. Changes in elemental content during apoptotic cell death studied by electron probe X-ray microanalysis. *Exp. Cell. Res.* **1999**, *253*, 454–462. [CrossRef]

34. Ziegler, U.; Groscurth, P. Morphological features of cell death. *News Physiol. Sci.* **2004**, *19*, 124–128. [CrossRef] [PubMed]

35. Enari, M.; Sakahira, H.; Yokoyama, H.; Okawa, K.; Iwamatsu, A.; Nagata, S. A caspase-activated DNase that degrades DNA during apoptosis, and its inhibitor ICAD. *Nature* **1998**, *391*, 43–50. [CrossRef]

36. Redza-Dutordoir, M.; Averill-Bates, D.A. Activation of apoptosis signalling pathways by reactive oxygen species. *Biochim. Biophys. Acta* **2016**, *1863*, 2977–2992. [CrossRef]

37. Okamoto, A.; Tanaka, M.; Sumi, C.; Oku, K.; Kusunoki, M.; Nishi, K.; Matsuo, Y.; Takenaga, K.; Shingu, K.; Hirota, K. The antioxidant N-acetyl cysteine suppresses lidocaine-induced intracellular reactive oxygen species production and cell death in neuronal SH-SY5Y cells. *BMC Anesthesiol.* **2016**, *16*, 104. [CrossRef]

38. Liu, Z.; Zhou, T.; Ziegler, A.C.; Dimitrion, P.; Zuo, L. Oxidative Stress in Neurodegenerative Diseases: From Molecular Mechanisms to Clinical Applications. *Oxid. Med. Cell. Longev.* **2017**, *2017*, 2525967. [CrossRef]

39. Hwang, J.H.; Hwang, I.S.; Liu, Q.H.; Woo, E.R.; Lee, D.G. (+)-Medioresinol leads to intracellular ROS accumulation and mitochondria-mediated apoptotic cell death in Candida albicans. *Biochimie* **2012**, *94*, 1784–1793. [CrossRef]

40. Enogieru, A.B.; Haylett, W.; Hiss, D.C.; Bardien, S.; Ekpo, O.E. Rutin as a Potent Antioxidant: Implications for Neurodegenerative Disorders. *Oxid. Med. Cell. Longev.* **2018**, *2018*, 6241017. [CrossRef]

41. Genaro-Mattos, T.C.; Mauricio, A.Q.; Rettori, D.; Alonso, A.; Hermes-Lima, M. Antioxidant Activity of Caffeic Acid against Iron-Induced Free Radical Generation–A Chemical Approach. *PLoS ONE* **2015**, *10*, e0129963. [CrossRef]

42. Xu, D.; Hu, M.J.; Wang, Y.Q.; Cui, Y.L. Antioxidant Activities of Quercetin and Its Complexes for Medicinal Application. *Molecules* **2019**, *24*, 1123. [CrossRef] [PubMed]

43. Kim, D.W.; Lee, W.J.; Asmelash Gebru, Y.; Choi, H.S.; Yeo, S.H.; Jeong, Y.J.; Kim, S.; Kim, Y.H.; Kim, M.K. Comparison of Bioactive Compounds and Antioxidant Activities of Maclura tricuspidata Fruit Extracts at Different Maturity Stages. *Molecules* **2019**, *24*, 567. [CrossRef]

44. Chen, W.; Li, Y.; Bao, T.; Gowd, V. Mulberry Fruit Extract Affords Protection against Ethyl Carbamate-Induced Cytotoxicity and Oxidative Stress. *Oxid. Med. Cell. Longev.* **2017**, *2017*, 1594963. [CrossRef]

45. Tungmunnithum, D.; Thongboonyou, A.; Pholboon, A.; Yangsabai, A. Flavonoids and Other Phenolic Compounds from Medicinal Plants for Pharmaceutical and Medical Aspects: An Overview. *Medicines* **2018**, *5*, 93. [CrossRef] [PubMed]

46. Sunil, A.G.; Kesavanarayanan, K.S.; Kalaivani, P.; Sathiya, S.; Ranju, V.; Priya, R.J.; Pramila, B.; Paul, F.D.; Venkhatesh, J.; Babu, C.S. Total oligomeric flavonoids of Cyperus rotundus ameliorates neurological deficits, excitotoxicity and behavioral alterations induced by cerebral ischemic-reperfusion injury in rats. *Brain Res. Bull.* **2011**, *84*, 394–405. [CrossRef]

47. Molehin, O.R.; Adeyanju, A.A.; Adefegha, S.A.; Oyeyemi, A.O.; Idowu, K.A. Protective mechanisms of protocatechuic acid against doxorubicin-induced nephrotoxicity in rat model. *J. Basic Clin. Physiol. Pharmacol.* **2019**, *30*. [CrossRef] [PubMed]

48. Sahin, A.; Kursat Cingu, A.; Kaya, S.; Turkcu, G.; Ari, S.; Evliyaoglu, O.; Cinar, Y.; Turkcu, F.M.; Yuksel, H.; Murat, M.; et al. The protective effects of caffeic acid phenethyl ester in isoniazid and ethambutol-induced ocular toxicity of rats. *Cutan. Ocul. Toxicol.* **2013**, *32*, 228–233. [CrossRef] [PubMed]

49. Aziza, S.A.; Azab Mel, S.; El-Shall, S.K. Ameliorating role of rutin on oxidative stress induced by iron overload in hepatic tissue of rats. *Pak. J. Biol. Sci.* **2014**, *17*, 964–977. [CrossRef]

50. Schapira, A.H. Science, medicine, and the future: Parkinson's disease. *BMJ* **1999**, *318*, 311–314. [CrossRef]

51. Budihardjo, I.; Oliver, H.; Lutter, M.; Luo, X.; Wang, X. Biochemical pathways of caspase activation during apoptosis. *Annu. Rev. Cell Dev. Biol.* **1999**, *15*, 269–290. [CrossRef] [PubMed]

52. Shamas-Din, A.; Kale, J.; Leber, B.; Andrews, D.W. Mechanisms of action of Bcl-2 family proteins. *Cold Spring Harb. Perspect. Biol.* **2013**, *5*, a008714. [CrossRef]

53. Wada, T.; Penninger, J.M. Mitogen-activated protein kinases in apoptosis regulation. *Oncogene* **2004**, *23*, 2838–2849. [CrossRef]

54. Soares-Silva, M.; Diniz, F.F.; Gomes, G.N.; Bahia, D. The Mitogen-Activated Protein Kinase (MAPK) Pathway: Role in Immune Evasion by Trypanosomatids. *Front. Microbiol.* **2016**, *7*, 183. [CrossRef]

55. Munoz, L.; Ralay Ranaivo, H.; Roy, S.M.; Hu, W.; Craft, J.M.; McNamara, L.K.; Chico, L.W.; Van Eldik, L.J.; Watterson, D.M. A novel p38 alpha MAPK inhibitor suppresses brain proinflammatory cytokine up-regulation and attenuates synaptic dysfunction and behavioral deficits in an Alzheimer's disease mouse model. *J. Neuroinflamm.* **2007**, *4*, 21. [CrossRef] [PubMed]

56. Borsello, T.; Forloni, G. JNK signalling: A possible target to prevent neurodegeneration. *Curr. Pharm. Des.* **2007**, *13*, 1875–1886. [CrossRef]

57. Lee, S.; Hoang, G.D.; Kim, D.; Song, H.S.; Choi, S.; Lee, D.; Kang, K.S. Efficacy of Alpinumisoflavone Isolated from Maclura tricuspidata Fruit in Tumor Necrosis Factor-alpha-Induced Damage of Human Dermal Fibroblasts. *Antioxidants* **2021**, *10*, 514. [CrossRef] [PubMed]

58. Hiep, N.T.; Kwon, J.; Hong, S.; Kim, N.; Guo, Y.; Hwang, B.Y.; Mar, W.; Lee, D. Enantiomeric Isoflavones with neuroprotective activities from the Fruits of Maclura tricuspidata. *Sci. Rep.* **2019**, *9*, 1757. [CrossRef]

59. Tilstra, J.S.; Clauson, C.L.; Niedernhofer, L.J.; Robbins, P.D. NF-kappaB in Aging and Disease. *Aging Dis.* **2011**, *2*, 449–465.

60. Lingappan, K. NF-kappaB in Oxidative Stress. *Curr. Opin. Toxicol.* **2018**, *7*, 81–86. [CrossRef]

61. Shen, Q.; Zhang, B.; Xu, R.; Wang, Y.; Ding, X.; Li, P. Antioxidant activity in vitro of the selenium-contained protein from the Se-enriched Bifidobacterium animalis 01. *Anaerobe* **2010**, *16*, 380–386. [CrossRef] [PubMed]